Acknowledgment

These investigations were supported by the Koninklijke/Shell Laboratorium, Amsterdam, The Netherlands. We also acknowledge W. Leppink for the construction of the experimental setup and C. van der Beek, W. Lengton, and G. Oudendijk for their part in the experimental work.

Nomenclature

C = concentration, mol m^{-3}
D = diffusivity, m^2 s^{-1}
E = enhancement factor
J = mole flux, mol m^{-2} s^{-1}
k_g = gas-phase mass-transfer coefficient, m s^{-1}
k_L = liquid-phase mass-transfer coefficient, m s^{-1}
m = dimensionless solubility
t = time variable, s
T = temperature, K
x = space variable, m

Subscripts/Superscripts

bulk = bulk conditions
calc = calculated
exp = experimental
i = component i
int = interfacial
g = gas phase
L = liquid phase
tot = total (i.e., free and converted)

Amine Abbreviations

DEMEA = diethylmonoethanolamine
MDEA = *N*-methyldiethanolamine
MMEA = methylmonoethanolamine
R_3N = tertiary amine

Registry No. MDEA, 105-59-9; DEMEA, 100-37-8; COS, 463-58-1.

Literature Cited

Al-Ghawas, H. A.; Sandall, O. C. Simultaneous absorption of carbon dioxide, carbonyl sulfide and hydrogen sulfide in aqueous methyldiethanolamine. *Chem. Eng. Sci.* **1991**, *46*, 665–676.

Al-Ghawas, H. A.; Ruiz-Ibanez, G.; Sandall, O. C. Absorption of carbonyl sulfide in aqueous methyldiethanolamine. *Chem. Eng. Sci.* **1989**, *44*, 631–639.

Blauwhoff, P. M. M.; Versteeg, G. F.; van Swaaij, W. P. M. A study on the reaction between CO_2 and alkanolamines in aqueous solutions. *Chem. Eng. Sci.* **1984**, *39*, 207–225.

Cornelisse, R.; Beenackers, A. A. C. M.; van Beckum, F. P. H.; van Swaaij, W. P. M. Numerical calculation of simultaneous mass transfer of two gases accompanied by complex reversible reactions. *Chem. Eng. Sci.* **1980**, *35*, 1245–1260.

Littel, R. J.; Filmer, B.; Versteeg, G. F.; van Swaaij, W. P. M. Modelling of simultaneous absorption of H_2S and CO_2 in alkanolamine solutions: The influence of parallel and consecutive reversible reactions and the coupled diffusion of ionic species. *Chem. Eng. Sci.* **1991**, *46*, 2303–2313.

Littel, R. J.; Versteeg, G. F.; van Swaaij, W. P. M. Solubility and diffusivity data for the absorption of COS, CO_2, and N_2O in amine solutions. *J. Chem. Eng. Data* **1992a**, *37*, 49–55.

Littel, R. J.; Versteeg, G. F.; van Swaaij, W. P. M. Kinetic study of COS with tertiary alkanolamine solutions. 1. Experiments in an intensely stirred batch reactor. *Ind. Eng. Chem. Res.* **1992b**, preceding paper in this issue.

Littel, R. J.; Versteeg, G. F.; van Swaaij, W. P. M. On the kinetics of COS with primary and secondary amines in aqueous solutions. *AIChE J.* **1992c**, in press.

Littel, R. J.; Versteeg, G. F.; van Swaaij, W. P. M. Kinetics of CO_2 with primary and secondary amines in aqueous solutions—I: Zwitterion deprotonation kinetics for DEA and DIPA in aqueous blends of alkanolamines. *Chem. Eng. Sci.* **1992d**, in press.

Philipp, B.; Dautzenberg, H. Kinetische Untersuchungen zur Bildung und Zetsetzung von Monothiocarbonat in wässrige Lösung. *Z. Phys. Chem.* **1965**, *229*, 210–224.

Versteeg, G. F.; van Swaaij, W. P. M. On the kinetics between CO_2 and alkanolamines both in aqueous and non-aqueous solutions—II: Tertiary amines. *Chem. Eng. Sci.* **1988a**, *43*, 587–591.

Versteeg, G. F.; van Swaaij, W. P. M. Solubility and diffusivity of acid gases (CO_2, N_2O) in aqueous alkanolamine solutions. *J. Chem. Eng. Data* **1988b**, *33*, 29–34.

Versteeg, G. F.; Oyevaar, M. H. The reaction between CO_2 and diethanolamine at 298 K. *Chem. Eng. Sci.* **1989**, *44*, 1264–1268.

Versteeg, G. F.; Kuipers, J. A. M.; van Beckum, F. P. H.; van Swaaij, W. P. M. Mass transfer with complex reversible chemical reactions—I: Single reversible chemical reactions. *Chem. Eng. Sci.* **1989**, *44*, 2295–2310.

Received for review July 25, 1991
Revised manuscript received January 30, 1992
Accepted February 5, 1992

Steam Gasification of Lignocellulosic Residues in a Fluidized Bed at a Small Pilot Scale. Effect of the Type of Feedstock

Javier Herguido, José Corella,* and José González-Saiz

Chemical and Environmental Engineering Department, University of Zaragoza, 50009 Zaragoza, Spain

Different biomass materials such as pine sawdust, pine wood chips, cereal straw, and thistles (*Cynara cardunculus*) from energetic crops have been gasified with steam in a 15-cm-i.d. fluidized bed reactor. The gas, tar, and char yields, the composition and heating value of the gas produced, and the conversion of carbon have been determined at temperatures between 650 and 780 °C (923–1053 K) for each material. The product distribution varies with the biomass used and the gasification temperature. The differences are very marked for the H_2, CO, and CO_2 contents in the gas product at low gasification temperatures. These differences decrease when the temperature increases to 780 °C at which point a gas composition similar for all types of biomass tested is obtained by the achievement of equilibrium in the water-gas shift reaction.

Introduction

The gasification of biomass, lignocellulosic residues, refuse derived fuel (RDF), organic wastes, etc., is a thermochemical process for destruction of such solids with simultaneous production of a valuable gas. Today it seems to be not economically competitive, and research on it has ceased in some laboratories. Nevertheless in some scenarios it could be attractive. The state of the art and its

0888-5885/92/2631-1274$03.00/0 © 1992 American Chemical Society

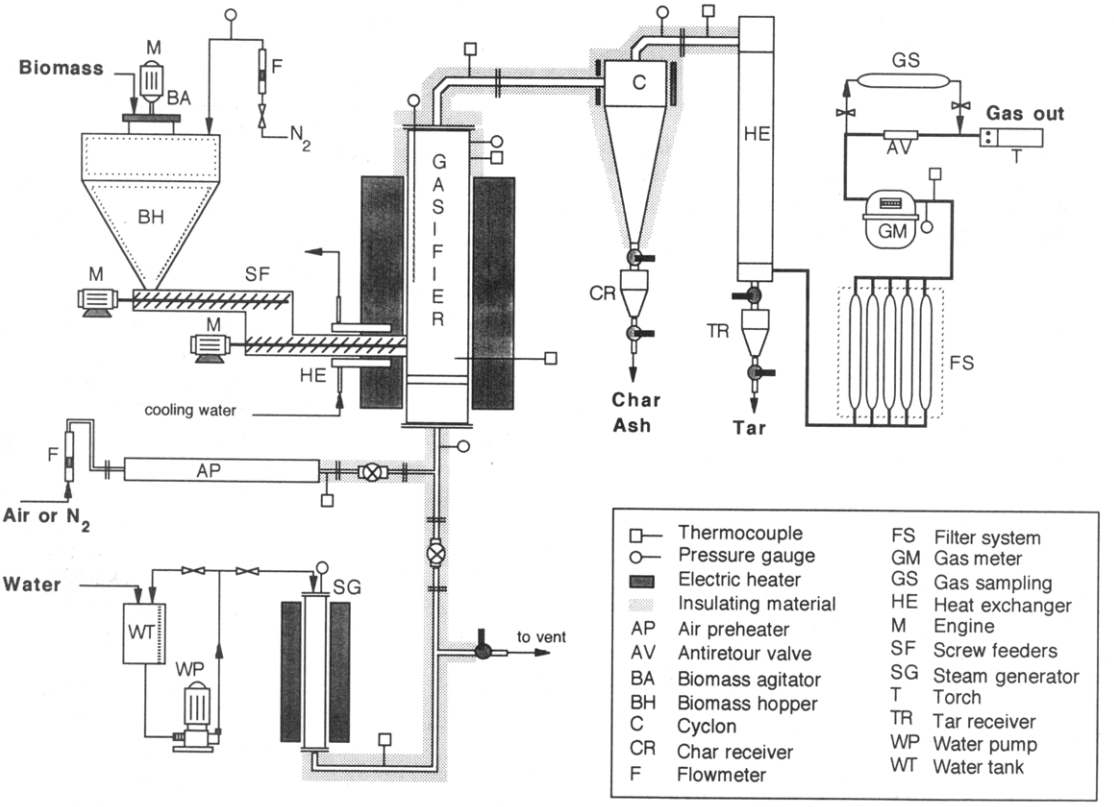

Figure 1. Scheme of the experimental installation.

future have been analyzed by Mendis (1989), Beenackers and Bridgwater (1989), and Beenackers and Van Swaaij (1990).

The most common gasification agent today is air, and the most promising technologies involve fluidized beds (bubbling, circulating, etc.). But air gasification has already been well-studied and it is well-known. Thus this work will be centered on steam gasification (without oxygen) in a bubbling fluidized bed. One operation variable not well-known in this process is the type of feedstock. A same gasifier should process different feedstocks generated or produced in the surroundings. Therefore, we considered it necessary to know how the product distribution changes when changes occur in the feedstock type being processed. Perhaps, product distribution can be correlated, in the future, with the feedstock composition given by several lumps (cellulose, hemicellulose, lignin, ash, etc.). But in the cracking of heavy oil feedstocks (FCC process), the interactions between the lumps which form the oil are so complex that, even after many years of research in such subject, it is very difficult to relate the product distribution with the oil composition. Since pyrolysis and cracking are very similar, and since biomass and organic residues are even more complex materials than oil, such correlation would be very difficult and questionable and it is beyond the scope of our study.

After the pioneering relevant, and fundamental studies in pyrolysis and gasification of biomass from the late 1970s and early 1980s of Antal (1981, 1982), Shafizadeh (1982), Rensfelt et al. (1978), etc., much work has been made in this field. For instance, Scott and Piskorz studied flash pyrolysis in a fluidized bed of maple, poplar bark, bagasse, wheat straw, etc. (Scott et al., 1985; Scott and Piskorz, 1982, 1984; Piskorz et al., 1986a,b). Also Nunn et al. (1985) reviewed the people who have studied the pyrolysis of different types of biomass. But these works were mainly for biomass pyrolysis, not for steam gasification in fluidized bed. Gasification of different biomasses was studied by

Table I. Gasifier Operating Conditions

reactor temperature range	650–780 °C (923–1053 K)
fluidizing gas mixture	90%/10% H_2O/N_2
superficial gas velocity at inlet (u_0)	0.25 m/s (at reactor temperature)
bed height at t = 0 and u_0 = u_{mf} (H_0)	0.32 m
total pressure in the gasifier	1.1 atm
steam/biomass ratio	0.8 (interval studied: 0.4–3.0)
second or fluidizing solid	silica sand from beach (≈8 kg) d_p = −300 + 200 μm u_{mf} = 6 cm/s u_{cf} = 11 cm/s

	flow rates			
	650 °C	700 °C	750 °C	780 °C
biomass (kg/h)	3.94	3.71	3.56	3.46
steam (kg/h)	3.39	3.22	3.06	2.98
nitrogen (Nm^3/h)	0.47	0.43	0.42	0.40
N_2 purge (Nm^3/h)	0.03	0.03	0.03	0.03

Kuester et al. (i.e. Prasad and Kuester, 1988) using a dual fluidized bed gasification system and by Walawender and Fan of the Kansas State University. These authors studied steam gasification in a 5-cm-i.d. fluidized bed of cotton wood branches (Singh et al., 1986), of pure cellulose (Wallawender et al., 1985), and of dried feedlot manure (Raman et al., 1980). Their work was very interesting and useful for us. Nevertheless, in our region the most common and abundant biomasses are different from the ones they used. We are going thus to give more information on steam gasification of biomass than was previously available and new data on the effect of biomass type, including types of practical interest for us. To make more realistic the scaling-up of these results, the work is made on a small pilot plant scale, in a 15-cm-i.d. fluidized bed gasifier, at temperatures between 650 and 780 °C. This study is only a part of a big project made at the University of Saragossa (Spain) on catalytic/two-stage gasification in a fluidized bed (Corella et al., 1991; Aznar et al., 1992) and in a

multisolid circulating double fluid bed (Herguido et al., 1991).

Experimental Facility

The installation used in this work is shown in Figure 1, and its main operating conditions are shown in Table I. The reactor or gasifier is a 15-cm-i.d. fluidized bed of 1.2-m total height and is made of a refractory steel. Under the gas distributor plate there is a zone of 15-cm height with ceramic rings for the final preheating of the gas. The gas distributor was made of special nozzles (22 nozzles of 25-mm diameter, with 10 orifices of 1-mm diameter each) embedded in a base of 1-cm tickness. This plate distributes the gas very well along the bed diameter and gives small bubbles and a very low pressure drop. Its good functioning has really been of key importance in the progress of this research.

The stationary bed, 32-cm height (at $u_0 = u_{mf}$ and at $t = 0$), was of silica sand (from beach) of −300 + 200 μm (u_{mf} = 7 cm/s, u_{cf} = 11 cm/s, with air at 750 °C; Aznar et al., 1988a; Delgado et al., 1991). The biomass or residue feeding point was at the lower part of the bed, 5 cm above the gas distributor. This feeding at the bed bottom is also fundamental so that the biomass or residue really enters into the bed. In fact, the char produced from the biomass or the solid waste segregates at the top of the bed because of its lesser density (Aznar et al., 1989). So, when the biomass or the residue is fed from above to the bed surface, the biomass and the produced tars could not really enter into the bed. In this case the heating rate of the incoming solid is less and its contact with the hot sand worse. Therefore, in that case the produced tars crack to a lesser extent than when the biomass or residue really enters into the bed, and a lower gas yield and a higher tar yield are thus obtained (Corella et al., 1988).

The feeding of the biomass to the gasifier is carried out continuously, at a prefixed and constant flow rate. This operation is not easy due to the characteristics (shape, size, easy pyrolysis, etc.) of the cellulosic residues and the high temperature of the gasifier. Our feeding system consists of a N_2 pressurized hopper, for avoiding the return of the hot gas from the gasifier, and a first stainless steel screw feeder of 6-cm diameter. This first screw provides the desired biomass flow rate (regulating its speed). In series there is then a second and very rapidly rotating screw feeder which introduces the biomass quickly into the reactor, avoiding its pyrolysis in the screw. It also has a water-cooled jacket for avoiding the heating of the screw and of the cellulosic waste by the adjacent and hot gasifier, which would pyrolyze the biomass in the same (with the resulting jamming). This feeding system has functioned well, but it has at least two limitations: (i) the relatively small size of the hopper does not allow runs of over 4 h, and (ii) the diameter of the screw (6 cm) does not allow for using cellulosic wastes of over 2-cm length, approximately.

The gasifier is heated by an external electric oven connected to a temperature controller. The installation has two lines in parallel for introducing the gasifying agent (steam) and other gases. The steam line is connected to a water tank, a membrane pump, and a steam generator (constituted by a bed heated by a external electric oven). The line for other gases (air, N_2, etc.) is provided with an electric preheater and the corresponding flow control devices.

The gas from the gasifier passes through a cyclone for separating the entrained fines (ash, char, sand), by a water-cooled heat exchanger in which steam and tars are condensed and by a demister consisting of five glass bulbs arranged in parallel and with a glass wool filling. After the continuous measurement of the gas flow, gas samples are taken and analyzed by gas chromatography (GC). The off (clean) gas is burnt in a torch.

The installation has two thermocouples in the reactor (bed axis and freeboard) and at other points (steam generator, gas preheater, reactor inlet, gas flow meter, etc.). Given that in the gasifier the bed was entirely fluidized ($u_0/u_{mf} \approx 4$ and $u_0/u_{cf} \approx 2.2$), there were not temperature gradients in it, as was confirmed by moving the thermocouple up and down along the bed axis. The bed temperature did not vary more than 10 °C along the length of the run. The temperatures given below should thus be understood as the averaged ones ± 10 °C, not more. The facility also had pressure probes at different points with a movable pressure probe at the gasifier top for determining the total bed height. The cyclone and the exit gas line, up to the heat exchanger, were externally heated with electrical resistances and insulated with a ceramic blanket. Their temperatures were always above 500 °C (793 K) for avoiding tar condensations and possible jams.

Procedure. Each run starts with the filling of the bed of silica sand. The minimum fluidization (u_{mf}) and complete fluidization (u_{cf}) velocities of the mixtures of this sand with different wastes and chars were previously determined in a auxiliary cold bed (Aznar et al., 1988a,b) and also at elevated temperatures (Delgado et al., 1991). Once the installation is hot, the steam is introduced at a prefixed superficial gas velocity (u_0), the cellulosic residue is fed, and the prefixed temperature in the bed is maintained with the external oven. At regular intervals of time, samples of gas and condensates are taken for their analysis by GC and by TOC (total organic carbon determination), respectively. The two-phase condensates are water-soluble and not-water-soluble species, light and heavy hydrocarbons and oxygenated compounds. We call both fractions tars. Although the water-soluble tar is a complex mixture of organic compounds, phenol will represent the "average" tar compound. The tar yield determination was made in the same manner as previously indicated by Sjöström et al. (1988), Aldén et al. (1988), and Corella et al. (1991).

Once the run was finished, the installation was cleaned, collecting the char and ash (in the bed and in the cyclone) and the condensed products. All products were measured, and mass balances were made. These balances were always quite satisfactory (always between 95–105%). The overall heat balance was not calculated given the difficulty of appraising the external energetic contribution given by the ovens and electrical resistances.

The condensed water and the tars were separated by distillation. The carbon content in the water-soluble tars was determined by a Dohrmann DC 90 TOC analyzer. The elementary analyses of the char and tars were carried out in a LECO CHN 600 analyzer. The gases were analyzed in a Hewlett-Packard 5710A chromatograph with a thermal conductivity detector (TCD). The components of interest include H_2, N_2, CO, CO_2, CH_4, C_2H_2, C_2H_4, and C_2H_6. The hydrogen was analyzed using a 5A molecular sieve column, with nitrogen as the carrier gas. The other components in the gas were analyzed with a Carbosieve 9A column with helium as carrier.

Operating Conditions. The main operation parameters are shown in Table I. The variables studied have been the feedstock type, gasification temperature, and steam/biomass ratio. The effect of the space–time (H_0/u_0, sometimes incorrectly called mean residence time) for the

Table II. Main Characteristics of Feedstocks

	sawdust	straw	wood chips	thistle
particle size	$\bar{d}_p \approx 500$ μm	$L > 5$ mm	$\bar{d} \approx 2 \times 5 \times 10$ mm	a
proximate analysis (wt % basis)				
moisture	8.5	7.8	11.1	10.0
ash	1.2	14.1	2.1	13.6
volatiles	77.4	61.6	74.4	60.7
fixed carbon	129	16.5	124	15.7
elemental analysis (% dry ash free basis)				
carbon	42.5	43.7	41.8	40.8
hydrogen	6.3	6.1	5.3	5.5
nitrogen	0.2	0.4	0.2	0.3
low heating value (MJ/kg of dry ash free biomass)	18.8	15.8	18.5	16.1

[a] Thistle is constituted of fibers and pith in different proportions; it is very difficult to give a medium particle size.

gas has already been previously studied (Corella et al., 1991).

To have a fully fluidized bed and to diminish the segregation of the char in the bed, according to Aznar et al. (1989), the superficial gas velocity at the bed inlet was approximately 4 times the u_{mf} of the sand.

Since u_0 or steam volumetric flow rate was maintained constant from one gasifier temperature to another and since the steam mass flow rate changes a little from one run to another, the biomass flow rate was varied a little (Table I) to have the same H_2O/biomass ratio.

Feedstocks. Four different cellulosic wastes have been processed. Pine (Pinus pinaster (*P. pinaster*)) sawdust was the most used given its easy feeding and processing (particles homogeneous in size and shape). The second biomass used was small pine (*P. pinaster*) wood chips with a small quantity of bark. The third was cereal (wheat) straw, one of the most abundant and available residues in Spain (it constitutes about 48% of the agricultural residues of this country). Its particles, once cut in a mill, had a flat form. Finally, thistles from energetic crops have been processed. They are a possible material for energetic use in the future given the high production per hectare and year in marginal lands. Two varieties are now being cultivated in Spain: *Onopordum nervosum* (*O. nervosum*) and *Cynara cardunculus* (*C. cardunculus*). In this work thistles of the *C. cardunculus* variety, triturated beforehand, have been gasified.

The pine sawdust and wood chips feedings did not give rise to any kind of problem. In the cases of the straw and thistles, given their fibrous form and their low density, they flow downward with difficulty, forming bridges and jams in the storage hopper. It was necessary thus to use a paddle agitator introduced vertically into the hopper to break the bridges and made the biomass fall to the feeding screw.

In Table II the main physicochemical properties of the cellulosic residues used are shown. More details about these solids concerning their fluid dynamics and processing in fluidized beds can be seen in the works of Aznar et al. (1988a,b). The four residues processed have a similar composition (dry-ash-free, Table II). The molecular formulas and the H/O ratio in the biomass (an important parameter according to Prasad and Kuester (1988)) of the four residues used are shown in Table III. They are based on the analysis of the same on a dry-ash-free basis.

Table III. Feedstocks Chemical Formula

	chemical formula: CH_xO_y		
feedstock	x	y	H/O
This Work			
wheat straw	1.675	0.613	2.734
Cynara thistles	1.607	0.733	2.193
pine sawdust	1.780	0.879	2.024
pine wood chips	1.521	0.908	1.676
Results of Prasad and Kuester (1988)			
guayule cork	1.726	0.356	4.841
Portuguese cork	1.725	0.397	4.345
shrub live oak	1.844	0.765	2.411
Euphorbia lathyris	1.983	0.902	2.200
sawdust	1.469	0.741	1.982
Russian thistle	1.979	1.081	1.831

Results and Discussion

Effect of the Steam Biomass Ratio. After each run the following was determined: (i) main product (gas, tar, char) distribution (after cleaning the installation and collecting all the products); (ii) exit gas composition (the averaged one for the different gas samples taken in an experiment); (iii) the gas heating value (expressed on a dry basis and free of nitrogen used as tracer and purge).

First, the effect of the steam/biomass ratio was studied. The gasification temperature in these experiments was always 750 °C and the biomass was pine sawdust. All other operation variables were the same as those indicated in Table I. The product distribution (gas, tar, char), gas composition, and low heating value of the gas are shown in Figure 2. A clear decrease of the tar yield with the steam/biomass ratio can be appreciated in Figure 2A (top, left). A steam/biomass ratio of about 0.80 was selected for further experiments.

Effect of the Gasification Temperature and of the Feedstock Type. Product Distribution. The gas yields at different gasification temperatures (T) for the different feedstocks are shown in Figure 3. Yield is defined in this figure as the kilogram of dry gas produced per kilogram of biomass fed. An important increase in the gas yield with the gasification temperature is observed, which agrees with what had been indicated in the literature with respect to this.

The increase of the gas yield with T is due first to the greater production of gas in the initial pyrolysis (faster at higher temperatures), second to the endothermal reactions of gasification of the char

$$C(s) + H_2O \rightleftarrows CO + H_2$$

$$C(s) + 2H_2O \rightleftarrows CO_2 + 2H_2$$

$$2C(s) + 2H_2O \rightleftarrows CH_4 + CO_2$$

$$C(s) + CO_2 \rightleftarrows 2CO$$

and third to the steam cracking and reforming of the tars, which increase with T, with the resulting increase of the gas yield.

The variation shown in Figure 3 agrees with the results of others in the bibliography. However, Wallawender et al. (1985) found inflection points in these curves which we do not observe. These authors found a first interval dominated by the cracking of the volatile matter and a second interval dominated by the shift reaction where the yield increase is less marked. This change of slope or of interval was at about 670 °C, a lower temperature than here used. For this reason observing such a change in our Figure 3 (if it really exists) is difficult.

The gas yield increases with T for all types of biomass, but important differences among some biomasses and others are observed, these differences being more pronounced at high temperatures. At 780 °C (1050 K), for

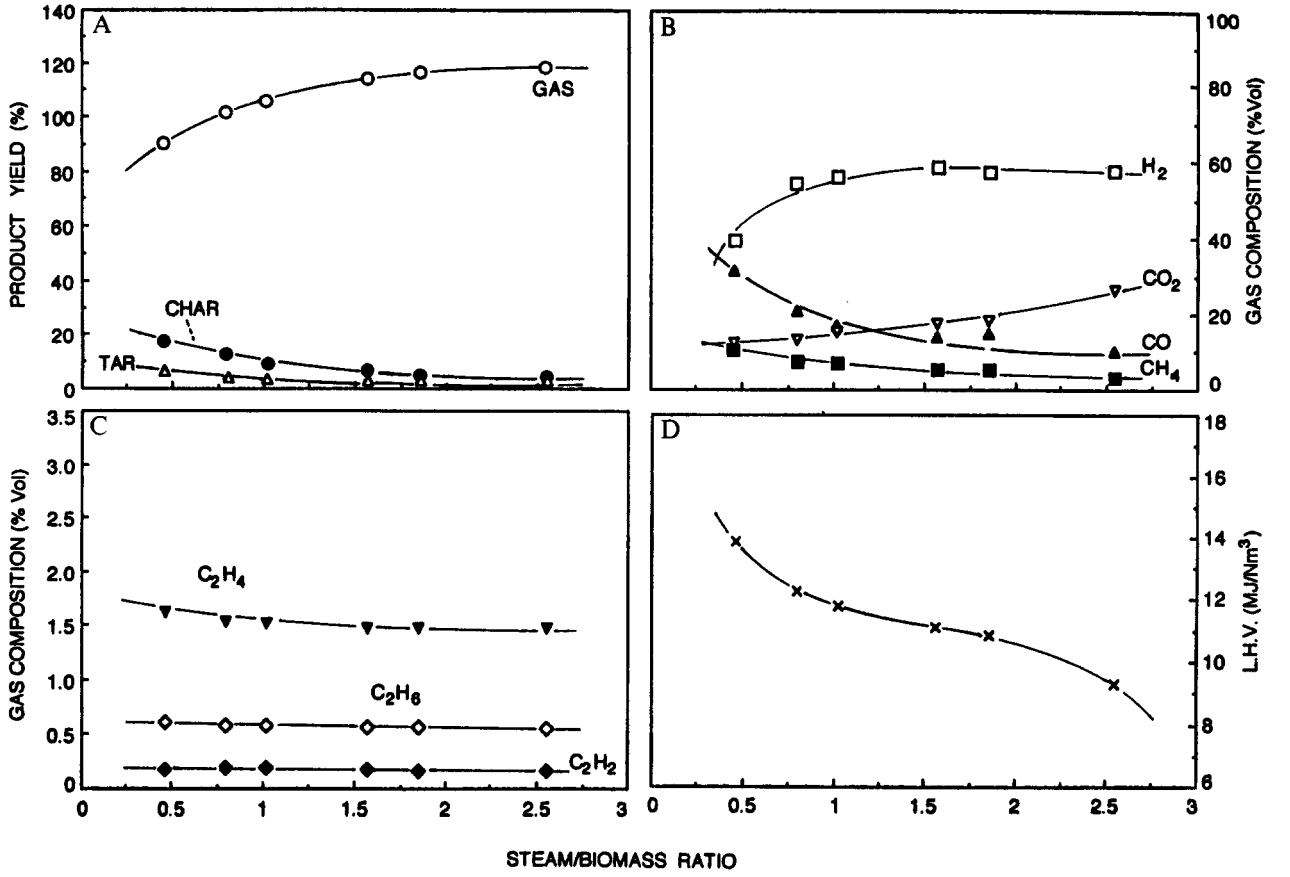

Figure 2. Effect of the steam/biomass ratio on the product distribution. Gasification of pine sawdust at T = 750 °C.

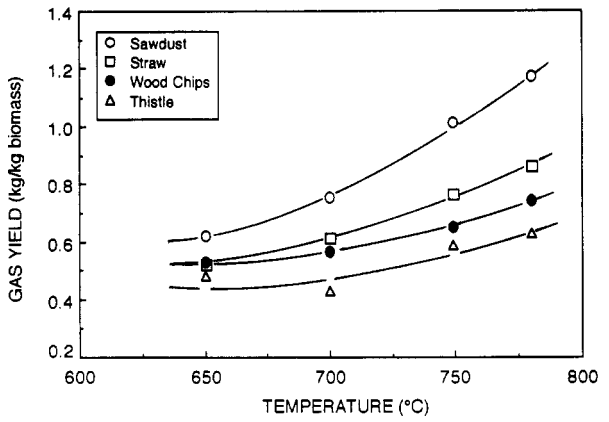

Figure 3. Gas yield vs temperature.

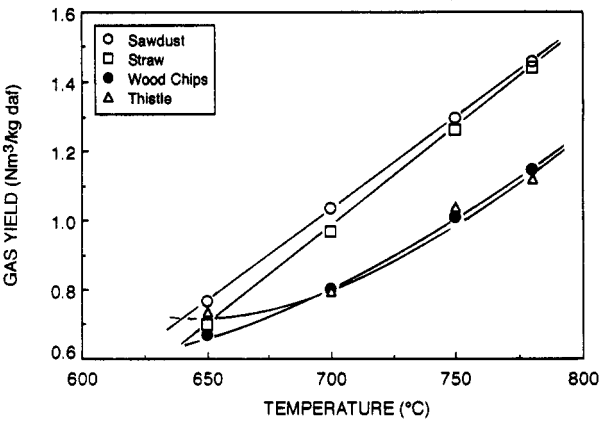

Figure 4. Gas yield (Nm^3) vs temperature.

example, the gas yield is of 1.2 kg of gas/kg of biomass for sawdust, while for thistles it is only 0.63 kg of gas/kg of biomass. We think this is due to the fact that in such definition of gas yield (kg of gas/kg biomass) the high content in inerts (ash) of biomasses such as straw and thistles (Table II) is included. This high content in ash means a high inert content in the biomass fed (with the corresponding decrease of gas yield).

The gas yield defined as the volume of gas produced per kilogram of biomass dry ash free is shown in Figure 4 at different gasification temperatures. Two groups of well-differentiated biomasses can be now observed: sawdust and straw on the one hand and chips and thistles on the other one. Sawdust and straw give a gas yield quite a lot higher than chips and thistles. Our explanation for this result is the following: attending to the content in volatiles of each biomass given in Table II, it would be expected that in the first stage of pyrolysis the gas production would be higher for the sawdust than for chips, and both higher than that from thistles and straw. In any case, the differences in gas yield would be less marked than those obtained experimentally. However, this difference is high. It can be attributed to the different sizes and shapes of the particles of each biomass used: in the first gasification step, pyrolysis, the size of the biomass already affects the production of gases. Beaumont and Schwob (1984), for instance, verify this influence, attributing it to the relation between the particle size and the heat transfer. This effect is more marked in the second step of char gasification with the steam and with the gases produced in the pyrolysis. For this step a shrinking-core model has been proposed, similar to that used for the coal char gasification (i.e. Chang, 1988). Char from the sawdust particles (big porosity and very small particle diameter) would have an effectiveness factor near unity. Char from chips has a surface/volume ratio much less and a lower porosity; it would have a lesser effectiveness factor. Thistles would have a similar factor. For the triturated straw, with a very

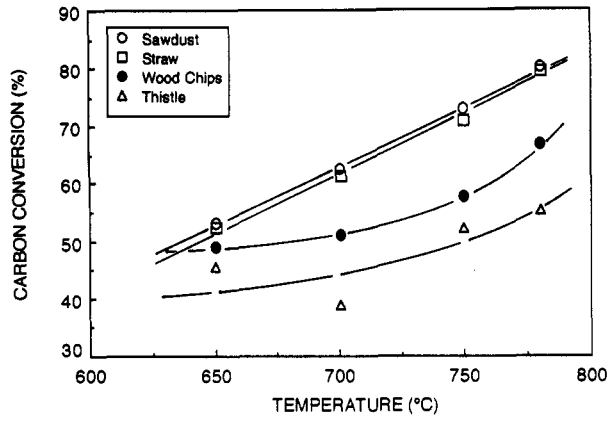

Figure 5. Carbon conversion vs temperature.

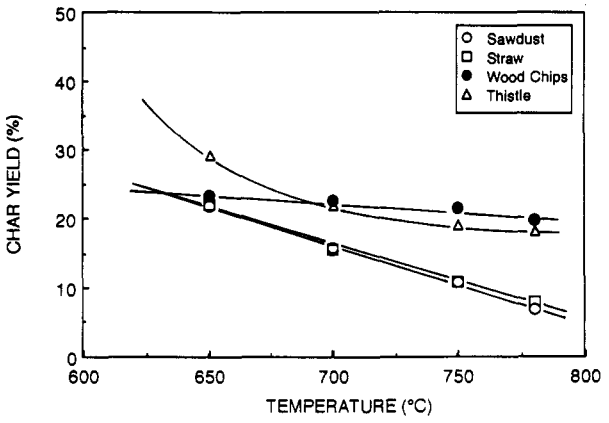

Figure 6. Char yield vs temperature.

small thickness, the preferential direction of the gasification reaction is the transverse one. Therefore, their effective size for the gasification is very small, and it has a similar behavior to that of the sawdust particles (effectiveness factor ≈1). The high gas yield obtained with the straw can also be explained by the catalytic effect of its ash, which has a high content in K_2O which favors the char-steam reaction.

Different ash contents in the biomass are important not only by their contribution in the overall weight of the biomass and by their further elimination from the flue gas but also by their relatively low melting point (presence of alkaline and alkaline-earth metals) and possibility of formation of eutectics with the walls, distributor plate, etc., of the gasifier. This fact can produce sintering or fusion in some parts of the gasifier above 800 °C, as once happened to us, with the straw.

Carbon Conversion. The percentage of carbon which passes from the biomass to the gas is shown in Figure 5. The results are in accordance with those just shown for the gas yield.

Char Production. Char yields, referred to the biomass dry ash free, for the four biomasses and at different temperatures, are shown in Figure 6. The decrease of the char yield with the gasification temperature was already known. Sawdust and straw are the biomasses which produce less char. This fact agrees with the greater gas yield that they give (Figure 4).

Tar Production. Tar yields are very similar for the different biomasses processed (Figure 7), and they decreased with the temperature, as was already known. The smaller production of tar occurs with the sawdust, the biomass that gives the greatest gas yield. Some of this gas would be thus originated from the cracking and reforming of the primary tars. A higher heating rate of the sawdust

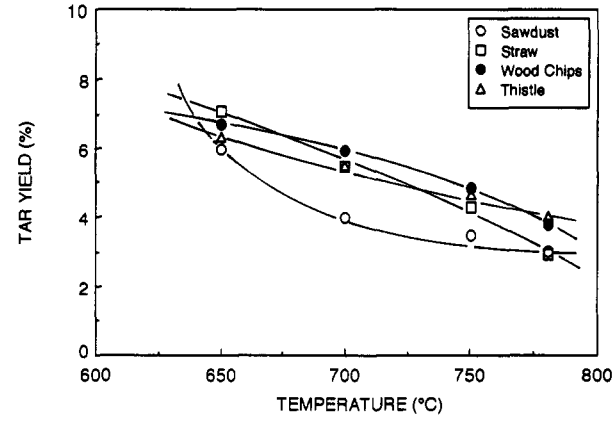

Figure 7. Tar yield vs temperature.

particles in the gasifier bed could be another reason for the low tar yield obtained.

The greater production of gases and the lesser one of tars in some biomasses, like oak samples, as opposed to others, like sugar cane bagasse, for Rodriguez et al. (1987), would be due to the lower porosity of the oak particles as opposed to the bagasse ones. This fact would make the tars remain a longer time in the particles of lower porosity. More tar would thus be cracked in the particle and converted into gases. This fact perhaps could contribute to the explanation of the difference shown in Figure 7 between sawdust and straw.

Exit Gas Composition. The main components in the dry-gas product, once the steam has been condensed in the heat exchanger, are H_2, CO, CO_2, and CH_4. Their contents are shown in Figure 8 for the different biomasses and gasification temperatures used.

Except for CH_4, whose content is practically the same (5–9%) for the four processed biomasses and whose variation with temperature is not very marked (Figure 8D), the other main components of the gas show a clear difference for the different biomasses used. This difference is important at low gasification temperatures and decreases with increasing temperature. At high temperature (780 °C) a similar gas composition is obtained (Figure 8A–C).

The yield of C_2 for the four biomasses is shown in Figure 9. More production of ethylene than of ethane and acetylene is observed. These yields vary very little with the gasification temperature.

Equilibrium in the Exit Gas. If above 940 K (670 °C) the shift reaction ($CO + H_2O \rightleftarrows CO_2 + H_2$) would dominate the process, the gas composition would be determined by this reaction. Different authors in gasification/gasifier modeling assume that this shift reaction is in equilibrium at the exit of the gasifier freeboard. Chang (1988), however, assumes that the equilibrium for the water-shift reaction is reached only at temperatures of the order of 1350 K. Maniatis and Buekens (1982) also obtained an important departure from the equilibrium in the exit gas (in the gasification of biomass in fluidized bed) at low temperatures.

The values of the $[H_2][CO_2]/[CO][H_2O]$ ratio ($=\varphi$) in the gasifier exit gas for each biomass are shown in Figure 10. The curve corresponding to the thermodynamic equilibrium constant is also shown there. These results are similar to those presented by Maniatis and Buekens (1982). The forward water-gas shift reaction has a kinetic constant (k_1) greater than the inverse reaction at temperatures below 810 °C (1083 K). At this temperature both kinetic constants (direct and inverse) are equal: K ($=\varphi_{theor}$) $= k_1/k_2 = 1$ (Figure 10, and also Prasad and Kuester (1988) and Walawender et al. (1985)). Note also how in our ga-

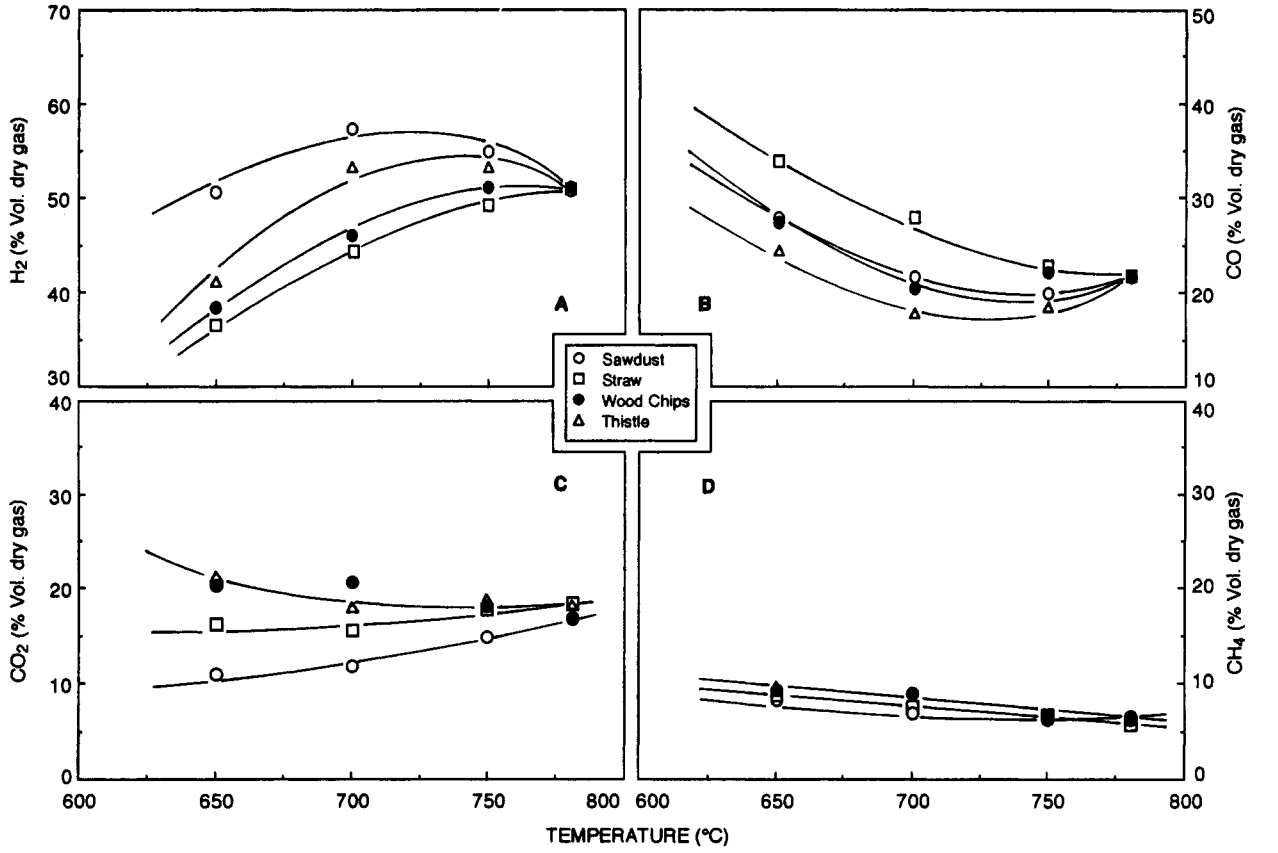

Figure 8. Effect of temperature on hydrogen (A), carbon monoxide (B), carbon dioxide (C), and methane (D) concentrations in the gas.

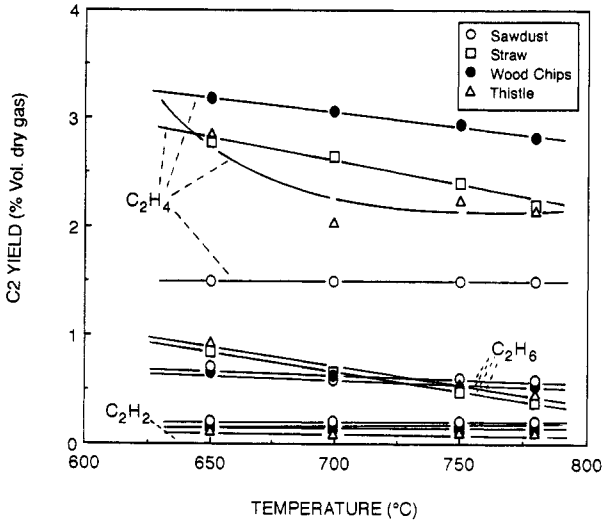

Figure 9. Effect of temperature on C_2 concentration in the product gas.

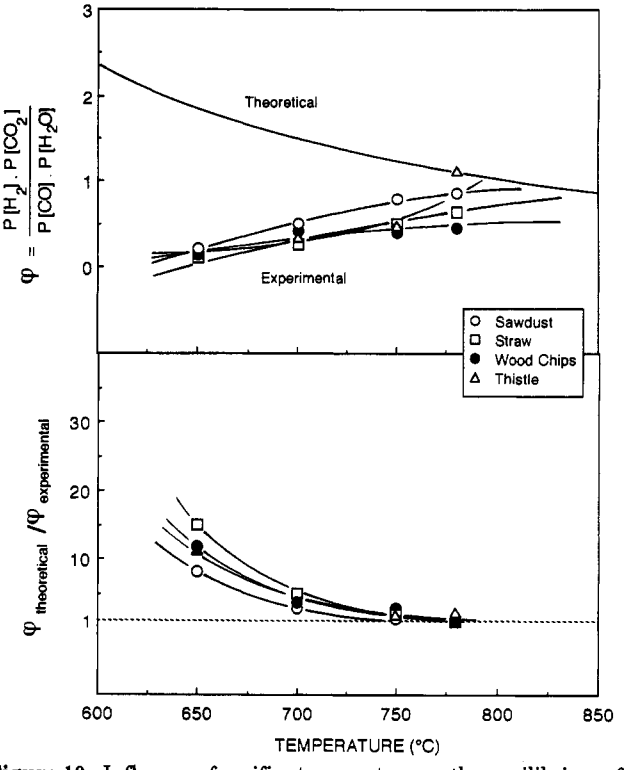

Figure 10. Influence of gasifier temperature on the equilibrium of the water-gas shift reaction (theoretical and experimental).

sifier the partial pressure of the steam (in the denominator of this ratio) is much greater than that of the other components (1.5–3 times greater than that of the H_2, which is the component in greatest proportion in the dry gas).

Our data show how the experimental values of the gas composition approach the equilibrium values above 750 °C (Figure 10). The $[H_2][CO_2]/[CO][H_2O]$ ratio comes near the theoretical one (given by equilibrium conditions). That means that on increasing T a progressive increase of the concentrations of H_2 and CO_2, and a decrease of that of CO, is obtained.

Walawender et al. (1985) used the slopes of the curves: "fraction in the gas produced of each component" vs temperature (between 940 and 1060 K). They consider that the variation of the slopes is only due to the shift reaction. If we compare the slopes they obtained with those obtained in this work (Table IV), some differences appear. These differences could be explained bearing in mind the existence, still significant, of other reactions, such as those of the char with the gases. Below 750 °C, considering only

Table IV. Slopes (1/K) in the Produced Gas Mole Fraction vs Temperature Curves (Averaged between 940 and 1060 K)

	slope × 10^4					
	Walawender et al. (1985)		this work			
component	theor	exptl	sawdust	straw	chips	thistle
H_2	5.63	4.75	7.2	13.7	9.7	10.9
CO_2	7.29	2.91	4.2	3.8	1.2	3.6
CO	-11.80	-5.11	-2.4	-0.9	-0.03	-1.9

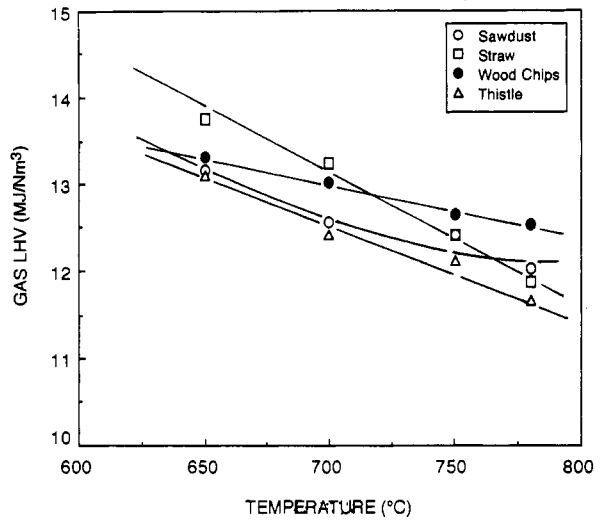

Figure 11. Low heating value of the dry gas vs temperature.

the shift reaction is not correct.

Gas Heating Value. The lower calorific value (LHV) of the gas produced (on a dry basis and free of N_2) at different gasification temperatures (T) is shown in Figure 11. A clear decrease of the LHV with T is observed. This decrease is compensated by a greater gas yield. Both effects make the energy in the gas phase per kilogram of processed biomass ratio increase with the gasification temperature.

Final Remarks. (i) With respect to CH_4 content in the exit gas, a small decrease with the operating temperature is observed, Figure 8D. CH_4 is not affected by the equilibrium of the water-shift reaction. CH_4 is produced by exothermic reactions of the type

$$C(s) + 2H_2 \rightleftarrows CH_4$$

$$CO + 3H_2 \rightleftarrows CH_4 + H_2O$$

whose equilibrium constant decreases with the temperature, meaning a decrease in the percentage of the CH_4 produced.

(ii) With respect to the relative values or percentage of each gaseous component in the gas mixture, for the different biomasses, the differences found are important at low gasification temperatures. Prasad and Kuester (1988) indicated that the H/O ratio in the biomass had some effect on the composition of the gas, obtaining higher H_2/CO ratios for growing values of the said ratio. With our experimental results at 650 and 780 °C, the following H_2/CO ratios are obtained:

	straw	thistle	sawdust	chips
H/O in biomass (Table III)	2.73	2.19	2.02	1.68
H_2/CO (650 °C)	1.10	1.69	1.79	1.35
H_2/CO (780 °C)	2.37	2.35	2.32	2.30

At a quite low temperature (650 °C) there is not a relation between the exit gas composition and the biomass composition. At 780 °C only a weak trend is observed.

On the other hand, the same as indicated by Prasad and Kuester (1988) and by Walawender et al. (1985), a maximum concentration of H_2 appears at 720–780 °C, depending on the biomass used.

(iii) Regarding the gasifier operation, the fluidization of all biomasses or lignocellulosic residues was feasible due to the fact that silica sand (of a correct size) was always used to fluidize them. The previous fluid-dynamic study of the sand–biomass, sand–char, dolomite–residues, etc., mixtures (Aznar et al., 1988a,b, 1989) was very important for the present study and process. We now think that the correct biomass/waste/residue processing/gasification/incineration is governed/controled by the hydrodynamic factors, not by the "kinetic" ones. Nearly all kinds of biomass/wastes/residues can be fluidized/processed/gasified/incinerated if they are milled under approximately 5-cm length and mixed with silica sand (or with dolomite, calcite, etc.) of a proper size.

(iv) In this work a low u_0 has been used (25 cm/s) which implied a low size for the silica sand. To increase the biomass throughput maintaining the steam/biomass ratio close to unity (Figure 2), a bigger steam flow rate, and hence u_0, should be used. Higher values for u_0 implies a higher u_{mf} (that is, a d_p) for the sand (to avoid its elutriation). Higher values for d_p of the sand than the ones used here have to be used thus in commercial fluidized bed gasifiers with high throughputs.

Conclusions

Very different biomasses and/or lignocellulosic residues can be gasified (or pyrolyzed, combusted, incinerated) in a fluidized bed (bubbling, circulating, etc.). They only need a previous crushing (trituration) to a size under about 5 cm and perhaps some kind of agitator in the biomass hopper (when it is too small in size) to break the bridges formed with some biomass like cereal straw and thistles. Silica sand (or dolomite, calcite, etc.) of a correct size has to be used in the gasifier as the supporting bed.

The gasification temperature is a parameter very important in the process. It determines the main product distribution and the gas composition. At low temperatures, under 750 °C, the exit gas composition is clearly different for each biomass. Above 750 °C the gas composition is near the same for all the biomass used. This gas composition is then governed by the water-shift reaction which attains the equilibrium in our gasifier freeboard. The CH_4 content (at 750–800 °C) in the exit gas is 5–7.5 vol %.

The size and shape of the biomass have influence on the product distribution. Small particle sizes (like the pine sawdust) or shapes near a plate (like the cereal straw) produce a greater gas yield and a lesser char yield than the bigger particles (chips).

Tar yields decrease with gasification temperatures and with the steam/biomass ratio. At 750–800 °C tar yields are between 2.8 and 5.0 wt %.

For the process to be carried out, the most important factors are perhaps the feeding system and the correct fluidization of the biomass (char)–silica sand (or dolomite) mixtures, which can easily be made. For further research in gasification pine sawdust is recommended as the feedstock which does not give special problems.

Acknowledgment

This work was carried out within the Shared Project between the CAICYT (Madrid) and the EEC (DG XII), Contract Nos. PB88-0391 and EN 3B-0103-E.

Nomenclature

d_p = mean particle diameter, μm
H_0 = bed height at $u_0 = u_{mf}$ and t = 0, cm

t = time on stream, h
u_{cf} = minimum fluidization velocity at which "all the bed" is fluidized, cm/s
u_{mf} = minimum fluidization velocity, cm/s
u_0 = superficial gas velocity at the bed inlet, cm/s

Registry No. H_2, 1333-74-0; CO, 630-08-0; CO_2, 124-38-9; C_2H_4, 74-85-1; C_2H_6, 74-84-0; C_2H_2, 74-86-2; CH_4, 74-82-8.

Literature Cited

Aldén, H.; Espenas, B. G.; Rensfelt, E. Conversion of Tar in Pyrolysis Gas from Wood using a Fixed Dolomite Bed. In *Research in Termochemical Biomass Conversion*; Bridgwater, A. V., Kuester, J. L., Eds.; Elsevier: London, 1988; pp 987–1001.

Antal, M. J. The Effect of Residence Time, Temperature, and Pressure on the Steam Gasification of Biomass. *Biomass as a Nonfossil Fuel Source*; American Chemical Society: Washington DC, 1981; Chapter 16.

Antal, M. J. Biomass Pyrolysis: a Review of the Literature. *Advances in Solar Energy*; American Solar Energy Society: New York, 1982; pp 61–111.

Aznar, M. P.; Grácia-Gorria, F. A.; Corella, J. u_{mf} and u_{cf} of Mixtures of Agricultural and Forestry Residues with a Second and Fluidizing Solid. Part I. *An. Quim. (Madrid)* **1988a**, *84*, 379–385 (*Int. Chem. Eng.* **1992**, *32* (1), 95–102.

Aznar, M. P.; Grácia-Gorria, F. A.; Corella, J. u_{mf} and u_{cf} of Mixtures of Agricultural and Forestry Residues with a Second and Fluidizing Solid. Part. II. *An. Quim. (Madrid)* **1988b**, *84*, 386–394 (*Int. Chem. Eng.* **1992**, *32* (1), 103–113.

Aznar, M. P.; Grácia-Gorria, F. A.; Corella, J. Segregation in the Fluidization of Mixtures of Forestry and Agricultural Residues with Silica Sand. *An. Quim. (Madrid)* **1989**, *85*, 100–108.

Aznar, M. P.; Corella, J.; Delgado, J.; Lahoz, J. Improved Steam Gasification of Cellulosic Residues in Fluidized Bed with Downstream Commercial Steam Reforming Catalysts. *Ind. Eng. Chem. Res.* **1992**, submitted for publication.

Beaumont, O.; Schwob, Y. Influence of Physical and Chemical Parameters on Wood Pyrolysis. *Ind. Eng. Chem. Process Des. Dev.* **1984**, *23*, 637–641.

Beenackers, A. A. C. M.; Bridgwater, A. V. *Gasification and Pyrolysis of Biomass in Europe*. In *Pyrolysis and gasification*; Ferrero, G. L., et. al., Eds.; Elsevier: London, 1989; pp 129–157.

Beenackers, A. A. C. M.; Van Swaaij, W. P. M. Gasification of Biomass. Needs for further R&D. In *Biomass for Energy and Industry*; Grassi, G., Gosse, G., dos Santos, G., Eds.; Elsevier: London, 1990; Vol 2, pp 2524–2533.

Chang, Y. H. A Mathematical Model for the Gasification of a Single Particle of Coal. *Int. Chem. Eng.* **1988**, *28*, 520–526.

Corella, J.; Herguido, J.; Alday, F. J. Pyrolysis and Steam Gasification of Biomass in Fluidized Bed. Influence of the Type and Location of the Biomass Feeding Point on the Product Distribution. In *Research in Thermochemical Biomass Conversion*; Bridgwater, A. V., Kuester, J. L., Eds.; Elsevier: London, 1988; pp 384–389.

Corella, J.; Aznar, M. P.; Delgado, J.; Aldea, E. Steam Gasification of Cellulosic Wastes in Fluidized Bed with Downstream Vessels. *Ind. Eng. Chem. Res.* **1991**, *30*, 2252–2262.

Delgado, J.; Corella, J.; Aznar, M. P.; Aragüés, J. L. u_{mf} at Elevated Temperatures in Coal/Biomass Gasifiers of Dolomite, Silica Sand and a Steam Reforming Catalyst. In *La Fluidisation*; Laguerie, C., Guigon, P., Eds.; Lavoisier: Paris, 1991; Vol. 5, No. 11, pp 62–69.

Herguido, J.; Corella, J.; Artal, G.; Garcia-Bordejé, E. Results with a Circulating Fluid Bed Pilot Plant for the Improved Steam Gasification of Biomass. In *Biomass for Energy, Industry and Environment*; Grassi, G., et al., Ed.; Elsevier: London, 1992; pp 792–796.

Maniatis, K.; Buekens, A. Fluidized Bed Gasification of Biomass. *EPE, Rev. Energ. Primaire* **1982**, *17* (3–4), 35–39.

Mendis, M. S. Biomass Gasification: Past Experiences and Future Prospects in Developing Countries. In *Pyrolysis and gasification*; Ferrero, G. L., et al., Eds.; Elsevier: London, 1989; pp 111–128.

Nunn, T. R.; Howard, J. B.; Longwell, J. P.; Peters, W. A. Product Compositions and Kinetics in the Rapid Pyrolysis of Sweet Gum Hardwood. *Ind. Eng. Chem. Process Des. Dev.* **1985**, *24*, 836–844.

Piskorz, J.; Scott, D. S.; Westerberg, I. B. Flash Pyrolysis of Sewage Sludge. *Ind. Eng. Chem. Process Des. Dev.* **1986a**, *25*, 265–270.

Piskorz, J.; Radlein, D.; Scott, D. S. On the Mechanism of the Rapid Pyrolysis of Cellulose. *J. Anal. Pyrolysis* **1986b**, *9*, 121–137.

Prasad, B. V. R.K.; Kuester, J. L. Process Analysis of a Dual Fluidized Bed Biomass Gasification System. *Ind. Eng. Chem. Res.* **1988**, *27*, 304–310.

Raman, K. P.; Walawender, W. P.; Fan, L. T. Gasification of Feedlot Manure in a Fluidized Bed Reactor. The Effect of Temperature. *Ind. Eng. Chem. Process Des. Dev.* **1980**, *19*, 623–629.

Rensfelt, E.; Blomkvist, G.; Ekstrom, C.; Engstrom, S.; Espenas, B. G.; Liinaki, L. Basic Gasification Studies for Development of Biomass Medium BTU Gasification Process. *IGT Conference on Energy from Biomass and Wastes*; Washington, DC, 1978.

Rodriguez, R.; Magne, P.; Deglixe, X. Sugar-Cane Bagasse as a Feedstock for an Industrial Fast Pyrolysis Process under Development. *J. Anal. Appl. Pyrolysis* **1987**, *12*, 301–318.

Scott, D. S.; Piskorz, J. The Fast Pyrolysis of Aspen-Poplar Wood. *Can. J. Chem. Eng.* **1982**, *60*, 666–674.

Scott, D. S.; Piskorz, J. The Continuous Flash Pyrolysis of Biomass. *Can. J. Chem. Eng.* **1984**, *62*, 404–412.

Scott, D. S.; Piskorz, J.; Radlein, D. Liquid Products from the Continuous Flash Pyrolysis of Biomass. *Ind. Eng. Chem. Process Des. Dev.* **1985**, *24*, 581–588.

Shafizadeh, F. Introduction of Pyrolysis of Biomass. Review. *J. Anal. Appl. Pyrolysis* **1982**, *3*, 283–305.

Singh, S. K.; Walawender, W. P.; Fan, L. T. Steam Gasification of Cottonwood (Branches) in a Fluidized Bed. *Wood Fiber Sci.* **1986**, *18*, 327–344.

Sjöström, K.; Taralas, G.; Liinaki, L. Sala Dolomite-Catalysed Conversion of Tar from Biomass Pyrolysis. In *Research in Thermochemical Biomass Conversion*; Bridgwater, A. V., Kuester, J. L., Eds.; Elsevier: London, 1988; pp 974–986.

Walawender, W. P.; Hoveland, D. A.; Fan, L. T. Steam Gasification of Pure Cellulose. 1. Uniform Temperature Profile. *Ind. Eng. Chem. Process Des. Dev.* **1985**, *24*, 813–817.

Received for review July 23, 1991
Revised manuscript received December 17, 1991
Accepted January 16, 1992